Journal of Achievements in Materials and Manufacturing Engineering
VOLUME 42
ISSUES 1-2
September-October
2010

Microstructure and mechanical properties of nanocomposite coatings deposited by cathodic arc evaporation

K. Lukaszkowicz [a,*], L.A. Dobrzański [a], W. Kwaśny [a], K. Labisz [a], M. Pancielejko [b]

[a] Division of of Materials Processing Technology, Management and Computer Techniques in Materials Science, Institute of Engineering Materials and Biomaterials, Silesian University of Technology, ul. Konarskiego 18a, 44-100 Gliwice, Poland

[b] Institute of Mechatronics, Nanotechnology and Vacuum Technique, Koszalin University of Technology, ul. Racławicka 15-17, 75-620 Koszalin, Poland

* Corresponding author: E-mail address: krzysztof.lukaszkowicz@polsl.pl

Received 13.04.2010; published in revised form 01.09.2010

Manufacturing and processing

ABSTRACT

Purpose: The main aim of the this research was the investigation of the structure and the mechanical properties of the nanocomposite TiAlSiN, CrAlSiN, AlTiCrN coatings deposited by cathodic arc evaporation method onto hot work tool steel substrate.

Design/methodology/approach: The surfaces' topography and the structure of the PVD coatings were observed on the scanning electron microscopy. Diffraction and thin film structure were tested with the use of the transmission electron microscopy. The microhardness tests were made on the dynamic ultra-microhardness tester. Tests of the coatings' adhesion to the substrate material were made using the scratch test.

Findings: It was found that the structure of the PVD coatings consisted of fine crystallites, while their average size fitted within the range of 11-25 nm, depending on the coating type. The coatings demonstrated columnar structure and dense cross-section morphology as well as good adhesion to the substrate. The critical load L_{C2} lies within the range of 46-54 N, depending on the coating and substrate type. The coatings demonstrate a high hardness (~40 GPa).

Practical implications: In order to evaluate with more detail the possibility of applying these surface layers in tools, further investigations should be concentrated on the determination of the thermal fatigue resistance of the coatings. The very good mechanical properties of the nanocomposite coatings make them suitable in industrial applications.

Originality/value: The investigation results will provide useful information to applying the nanocomposite coatings for the improvement of mechanical properties of the hot work tool steels.

Keywords: Thin&thick coatings; Nanostructure coatings, Microstructure, Mechanical properties

Reference to this paper should be given in the following way:

K. Lukaszkowicz, L.A. Dobrzański, W. Kwaśny, K. Labisz, M. Pancielejko, Microstructure and mechanical properties of nanocomposite coatings deposited by cathodic arc evaporation, Journal of Achievements in Materials and Manufacturing Engineering 42/1-2 (2010) 156-163.

1. Introduction

The research issues concerning the production of coatings is one of the more important directions of surface engineering development, ensuring the obtainment of coatings of high usable properties in the scope of mechanical characteristics and wear resistance. Giving new operating characteristics to commonly known materials is frequently obtained by laying simple monolayer, multilayer or gradient coatings using PVD methods [1-5]. While selecting the coating material, we encounter a barrier caused by the fact that numerous properties expected from an ideal coating is impossible to be obtained simultaneously. For example, an increase of hardness and strength causes the reduction of the coating's ductility and adherence to the substrate. The application of the nanostructure coatings is seen as the solution of this issue [6, 7]. According to the Hall-Petch equation, the strength properties of the material rise along with the reduction of the grain size. In case of the coatings deposited in the PVD processes, the structures obtained, with grain size ~10 nm cause the obtainment of the maximum mechanical properties. Coatings of such structure present very high hardness >40 GPa, ductility, stability in high temperatures, etc. [8-10]. The known dependency between the hardness and abrasion resistance became the foundation for the development of harder and harder coating materials. The progress in the field of producing coatings in the physical vapour deposition process enables the obtainment of coatings of nanocrystal structure presenting high mechanical and usable properties. The coatings of such structure are able to maintain a low friction coefficient (self-lubricating coatings) in numerous working environments, maintaining high hardness and increased resistance [11, 12]. The main concept in the achievement of high hardness of nanostructure coatings and good mechanical properties and high strength related to it, particularly in case of nanocomposite coatings [13-15] is the restriction of the rise and the movement of dislocations. High hardness and strength of the nanocomposite coatings are due to the fact that the movement of dislocations is suppressed at small grains and in the spaces between them, which causes the appearance of incoherent deformations. When the grain size is reduced to that of nanometers, the activity of dislocations as the source of the material ductility is restricted. This type of coatings is also characterized with a large number grain boundaries with a crystalline/amorphous transition across grain-matrix interfaces, restricting the rise and development of cracks. Such mechanism explains the resistance to fragile cracking of nanocomposite coatings [16-18]. Simultaneously, the equiaxial grain shapes, high angle grain boundaries, low surface energy and the presence of the amorphous boundary phase facilitating the slide along the grain boundaries causes a high plasticity of the nanocomposite coatings [6].

The purpose of this paper is to examine the microstructure and mechanical properties of nanocomposite coatings deposited by cathodic arc evaporation method on the X40CrMoV5-1 hot work tool steel substrate.

2. Investigation methodology

The tests were made on samples of the X40CrMoV5-1 hot work tool steel deposited by PVD process with TiAlSiN, CrAlSiN, AlTiCrN hard coatings.

Specimens were subjected to heat treatment consisting in quenching and tempering; austenizing was carried out in the vacuum furnace at 1020°C with a soaking time of 0.5 h. Two isothermal holds were used during heating up to the austenizing temperature, the first at the temperature of 640°C and the second at 840°C. The specimens were tempered twice after quenching, each time for 2 hours at the temperature of 560°C and next at 510°C. To ensure a proper quality, the surfaces of the steel specimens have been subjected to mechanical grinding and polishing (Ra=0.03 μm).

The coating deposition process was made in a device based on the cathodic arc evaporation method in an Ar and N2 atmosphere. Cathodes containing pure metals (Cr, Ti) and the AlSi (88:12 wt. %) alloy were used for deposition of the coatings. The base pressure was 5×10-6 mbar, the deposition temperature was approximately 500oC. The deposition conditions are summarized in Table 1.

Observations of surface and structures of the deposited coatings were carried out on cross sections in the SUPRA 35 scanning electron microscope. Detection of secondary electron was used for generation of fracture images with 15 kV bias voltage.

Diffraction and thin film structure were tested with the use of the JEOL JEM 3010UHR transmission electron microscope, at 300 kV bias voltage. Thin foils were made by mechanical grinding and further ion polished using the Gatan apparatus.

Phase identification of the investigated coatings was performed by glancing angle X-ray diffraction (GAXRD).

The cross-sectional atomic composition of the samples was obtained by using a glow discharge optical spectrometer, GDOS-750 QDP from Leco Instruments. The following operation conditions of the spectrometer Grimm lamp were fixed during the tests:

- lamp inner diameter-4 mm;
- lamp supply voltage-700 V;
- lamp current-20 mA;
- working pressure-100 Pa.

Tests of the coatings' adhesion to the substrate material were made using the scratch test on the CSEM REVETEST device. The tests were made using the following parameters:

- load range: 0-100 N,
- load increase rate (dL/dt): 100 $Nmin^{-1}$,
- indenter's sliding speed (dx/dt): 10 $mmmin^{-1}$,
- acoustic emission detector's sensitivity AE: 1.

The critical load LC, causing the loss of the coating adhesion to the material, was determined on the basis of the values of the acoustic emission, AE, and friction force, Ft, and observation of the damage developed in the track using a LEICA MEF4A optical microscope.

X-ray line broadening technique was used to determine crystallite size of the coatings using Scherrer formula with silicon as internal standard:

$D = (0.9\lambda/B\cos\theta_B)$

where:

D - crystallite size,

B - full width at half-maximum XRD peak in radians,

λ - wavelength of the X-ray radiation,

θ_B - the Bragg angle in radians.

The microhardness tests of coatings were made with the SHIMADZU DUH 202 ultra-microhardness tester. The test conditions were selected in order as to be comparable for all coatings. Measurements were made with 50 mN load, to eliminate the substrate influence on the coating hardness.

The thickness of coatings was determined using the ''kalotest'' method, i.e. measuring the characteristics of the spherical cap crater developed on the surface of the coated specimen tested.

Table 1.
Deposition parameters of the coatings

Coating	Substrate bias voltage [V]	Arc current source [A]	Pressure [Pa]
TiAlSiN	-90	Ti - 80 AlSi - 120	2.0
CrAlSiN	-60	Cr - 70 AlSi - 120	3.0
AlTiCrN	-60	Cr - 70 AlTi - 120	2.0

3. Discussion of results

The morphology of the coatings' surfaces deposited on the brass substrate is characterized by a significant inhomogeneity connected with occurrences of the multiple near-drop-shaped or close to spherical particles (Figs. 1-3), which is connected with the essence of the used cathodic arc evaporation process for depositing the coatings. Apart from single drops one can observe double particles and agglomerates created from several connected particles. Sizes of these particles are differentiated and are from several tenths to about 3 μm.

The coatings present a compact structure, without any visible delaminations or defects. The morphology of the fracture of coatings is characterized with a dense structure, in some cases there is a columnar structure (Figs. 4-6). The fractographic studies of the fractures of the steel samples examined, with the coatings deposited on their surface show a sharp transition zone between the substrate and the coating.

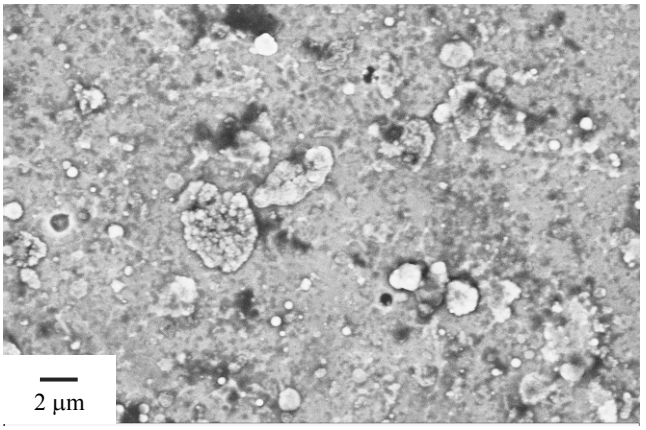

Fig. 2. Topography of the CrAlSiN coating surface deposited onto the X40CrMoV5-1 steel substrate

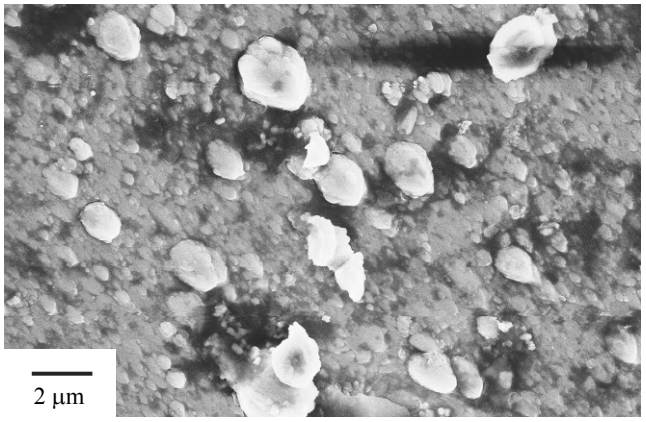

Fig. 1. Topography of the TiAlSiN coating surface deposited onto the X40CrMoV5-1 steel substrate

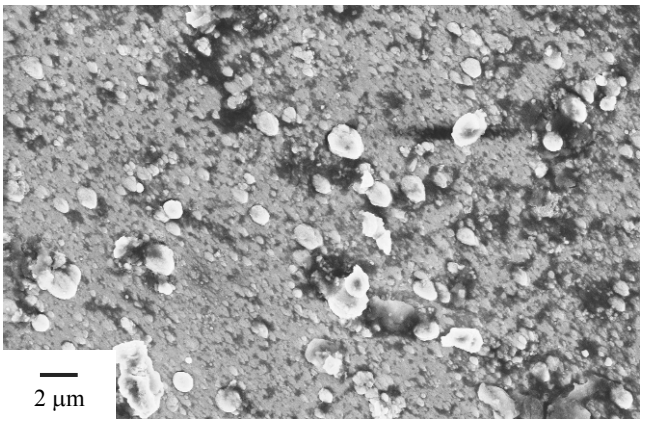

Fig. 3. Topography of the AlTiCrN coating surface deposited onto the X40CrMoV5-1 steel substrate

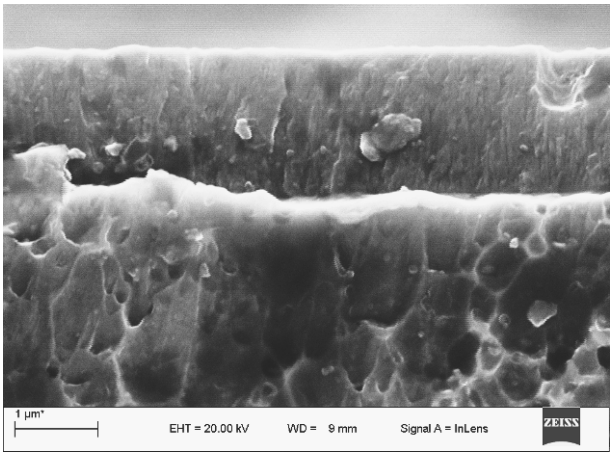

Fig. 4. Fracture of the TiAlSiN coating deposited onto the X40CrMoV5-1 steel substrate

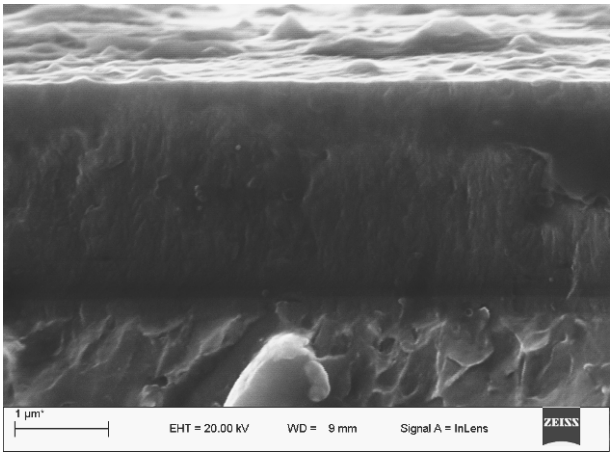

Fig. 5. Fracture of the CrAlSiN coating deposited onto the X40CrMoV5-1 steel substrate

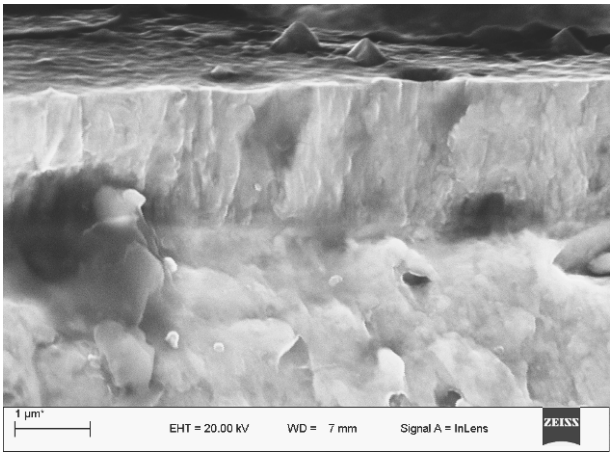

Fig. 6. Fracture of the AlTiCrN coating deposited onto the X40CrMoV5-1 steel substrate

In virtue of tests of coatings in a transmission electron microscope (TEM), it was observed that the coatings were built from fine crystallites. In general, there are no prerequisites whatsoever to suggest the epitaxial growth of the coatings examined. Single large grains were only observed in case of the TiAlSiN coating (Fig. 7), which may suggest the occurrence of the epitaxion phenomenon as the consequence of large crystallite occurrence in the coating.

Basing on the glancing angle X-ray diffraction (GAXRD) of the samples examined (Figs. 8-10), the occurrence of fcc phases was only observed in the coatings. The hexagonal AlN of wurtzite type was not discovered in the coatings examined, which could have been caused by a low amount of aluminium in the coatings. In case of the TiAlSiN coating a lattice parameter of 0.426 nm was derived, which is greater than that of bulk TiN (0.424 nm). The highest lattice parameter corresponds to a system where a partial Si segregation occurred, which might be enough to nucleate and develop a Si_3N_4 amorphous phase. Also, decrease intensities of the reflections, showing an increase in the amorphous content in the coatings. Basing on the results obtained, using Scherrer method, the size of crystallites in the coatings examined was determined. The results were presented in Table 2.

The hardness of the coatings tested fits within the range from 40 to 42 GPa. The highest hardness was recorded in the case of the AlTiCrN coating (Table 2).

Changes of coating component concentration and substrate material made in GDOS were presented in Figs. 11-13. The tests carried out with the use of GDOS indicate the occurrence of a transition zone between the substrate material and the coating, which results in the improved adhesion between the coatings and the substrate. In the transition zone between the coatings and the substrate the concentration of the elements of the substrate increases with simultaneous rapid decrease of concentration of elements contained in the coatings. The existence of the transition zone should be connected with the increase of desorption of the substrate surface and the occurrence of defects in the substrate and the relocation of the elements within the connection zone as a result of a high energy ion reaction. Such results, however, cannot be interpreted explicitly, due to the non-homogeneous evaporation of the material from the sample surface.

The critical load values L_{C1} and L_{C2} were determined by the scratch test method (Figs. 14-16). The load at which the first coating defects appear is known in the references [19, 20] as the first critical load L_{C1}. The first critical load L_{C1} corresponds to the point at which first damage is observed; the first appearance of microcraking, surface flaking outside or inside the track without any exposure of the substrate material - the first cohesion-related failure event. L_{C1} corresponds to the first small jump on the acoustic emission signal, as well as on the friction force curve. The second critical load L_{C2} is the point at which complete delamination of the coatings starts; the first appearance of cracking, chipping, spallation and delamination outside or inside the track with the exposure of the substrate material - the first adhesion-related failure event. After this point the acoustic emission graph and friction forces have a disturbed run (become noisier). The cumulative specification of the test results are presented in Table 2.

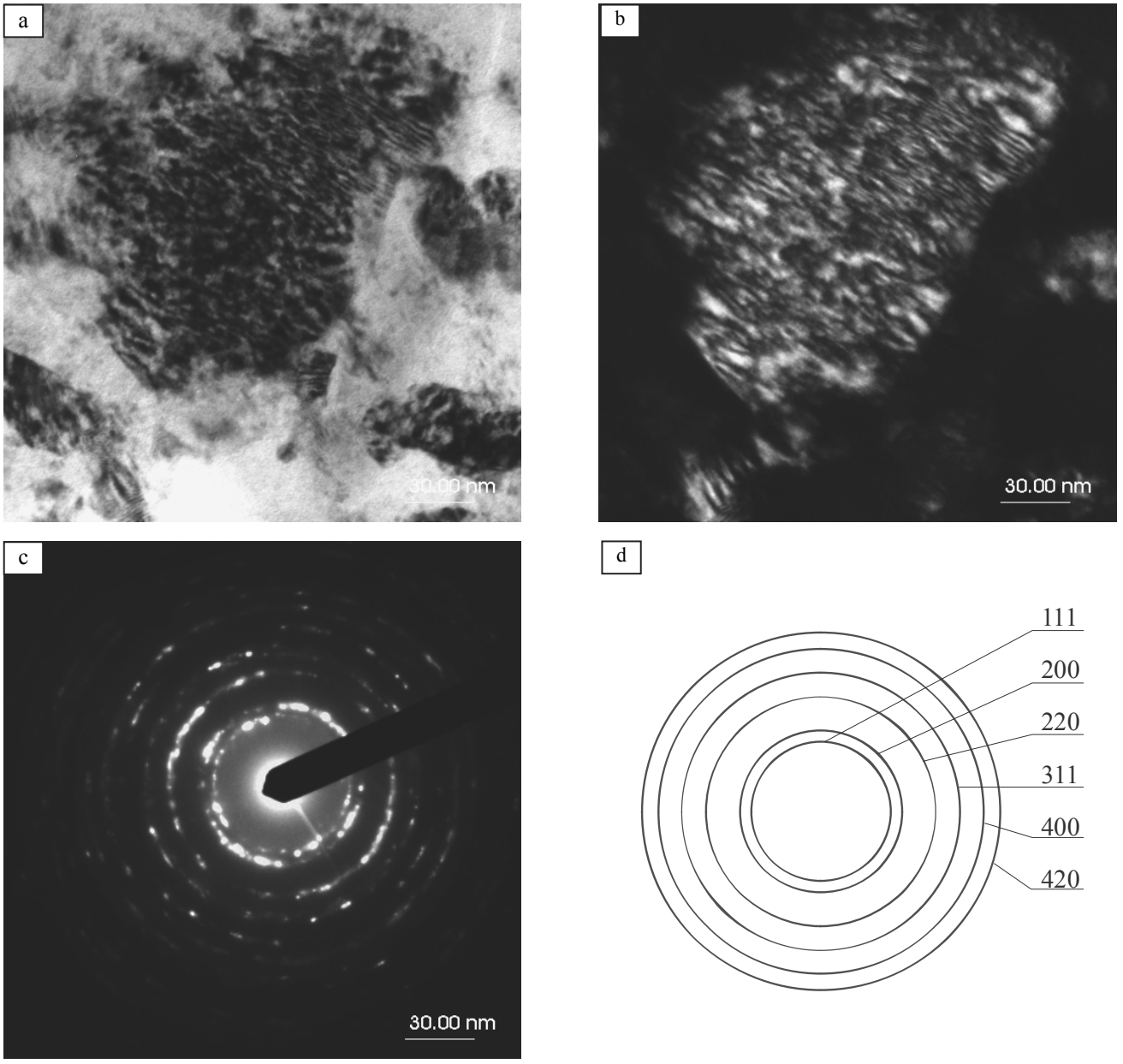

Fig. 7. Microstructure of the thin foil from the TiAlSiN coating, (a) light field, (b) dark field from the (111) reflex, (c) diffraction pattern from the area as in figure a, (d) solution of the diffraction pattern

Table 2.
The characteristics of the tested coatings

Coating	Thickness [μm]	Microhardness [GPa]	Crystallite size [nm]	Critical load L_{C1} [N]	Critical load L_{C2} [N]
AlTiCrN	2.4	42	17	24	54
CrAlSiN	2.9	40	25	18	49
TiAlSiN	2.1	40	11	16	46

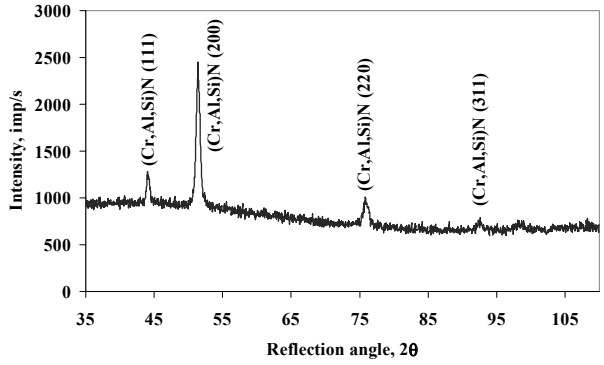

Fig. 8. GAXRD spectra of the CrAlSiN coating at glancing incidence angle α=2°

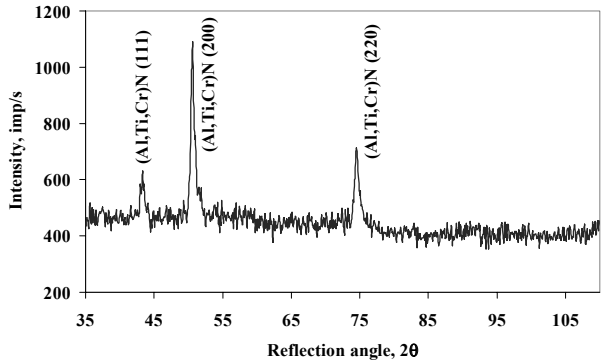

Fig 9. GAXRD spectra of the AlTiCrN coating at glancing incidence angle α=2°

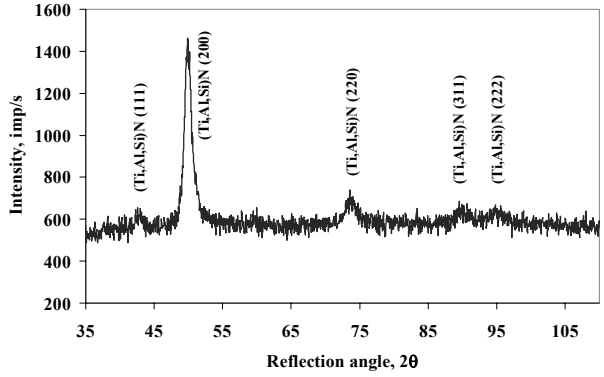

Fig. 10. GAXRD spectra of the TiAlSiN coating at glancing incidence angle α=2°

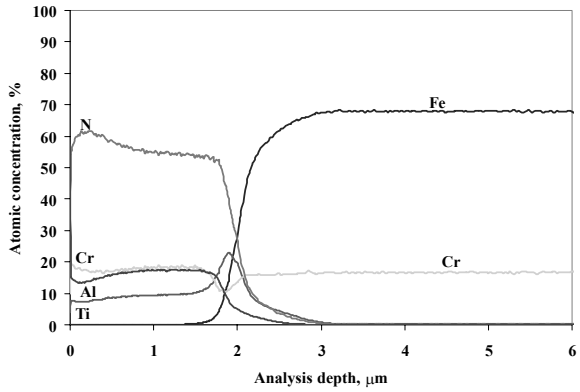

Fig. 11. Changes of constituent concentration of the AlTiCrN and the substrate materials

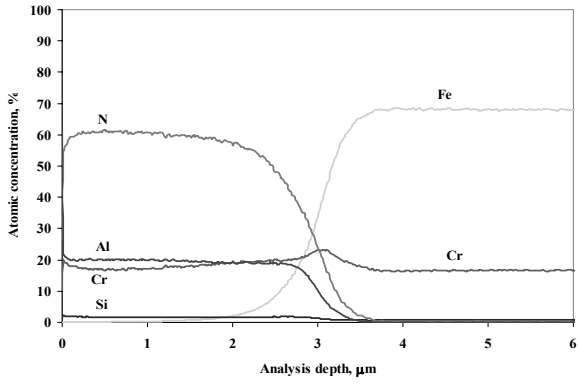

Fig. 12. Changes of constituent concentration of the CrAlSiN and the substrate materials

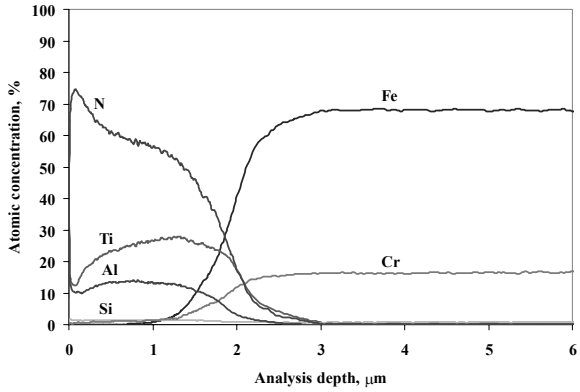

Fig. 13. Changes of constituent concentration of the TiAlSiN and the substrate materials

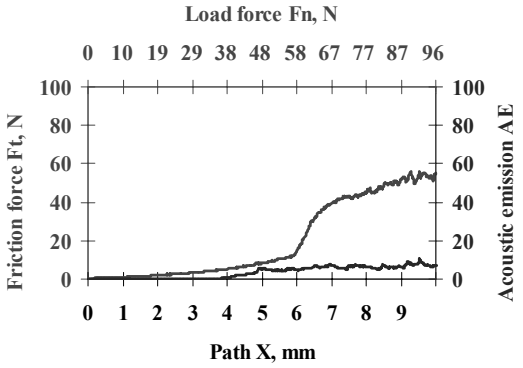

Fig. 14. Diagram of the dependence of the acoustic emission (AE) and friction force F_t on the load for the X40CrMoV5-1 steel with the AlTiCrN coating

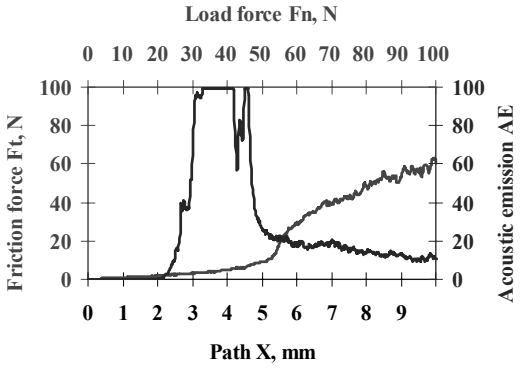

Fig. 15. Diagram of the dependence of the acoustic emission (AE) and friction force F_t on the load for the X40CrMoV5-1 steel with the CrAlSiN coating

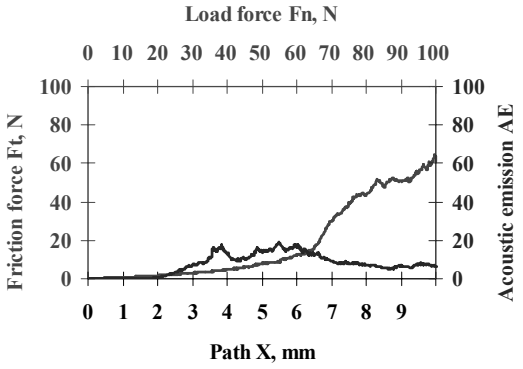

Fig. 16. Diagram of the dependence of the acoustic emission (AE) and friction force F_t on the load for the X40CrMoV5-1 steel with the TiAlSiN coating

In order to establish the nature of damage responsible for the occurring increase of the acoustic emission intensity, the cracks produced during the test were examined by the light microscope coupled with the measuring device, determining the critical load L_{C1} and L_{C2} in virtue of metallographic observations. In case of the coatings examined, it was found that coating AlTiCrN had the highest critical load value L_{C1}=24 N and L_{C2}=54 N.

4. Summary

The compact structure of the coatings without any visible delaminations was observed as a result of tests in the scanning electron microscope. The fracture morphology of the coatings tested is characterised with a dense structure. Basing on the thin film test in the transmission electron microscope, it was observed that the coatings are built of fine crystallites. Their size is 11-25 nm. The coating adhesion scratch tests disclose the cohesion and adhesion properties of the coatings tested. In virtue of the tests carried out, it was found that the critical load L_{C2} fitted within the range 46-54 N for the coatings deposited on a substrate made of hot work tool steel. The tests made with the use of GDOS indicate the occurrence of a transition zone between the substrate material and the coating, which affects the improved adhesion between the coatings and the substrate.

Acknowledgements

Research was financed partially within the framework of the Polish State Committee for Scientific Research Project No N N507 550738 headed by Dr Krzysztof Lukaszkowicz.

References

[1] L.A. Dobrzański, K. Lukaszkowicz, J. Mikuła, D. Pakuła, Structure and corrosion resistance of gradient and multilayer coatings, Journal of Achievements in Materials and Manufacturing Engineering 18 (2006) 75-78.

[2] L.A. Dobrzański, K. Lukaszkowicz, K. Labisz, Structure of monolayer coatings deposited by PVD techniques, Journal of Achievements in Materials and Manufacturing Engineering 18 (2006) 271-274.

[3] L.A. Dobrzański, M. Staszuk, A. Kriz, K. Lukaszkowicz, Structure and mechanical properties of PVD gradient coatings deposited onto tool steels and sialon tool ceramics, Journal of Achievements in Materials and Manufacturing Engineering 37 (2009) 36-43.

[4] M. Polok-Rubiniec, L.A. Dobrzański, K. Lukaszkowicz, M. Adamiak, Comparison of the structure, properties and wear resistance of the TiN PVD coatings, Journal of Achievements in Materials and Manufacturing Engineering 27 (2008) 87-90.

[5] L.A. Dobrzański, K. Lukaszkowicz, Mechanical properties of monolayer coatings deposited by PVD techniques, Archives of Materials Science and Engineering 28 (2007) 549-556.

[6] A.A. Voevodin, J.S. Zabinski, C. Muratore, Recent advances in hard, tough and low friction nanocomposite coatings, Tsinghua Science and Technology 10 (2005) 665-679.

[7] S.M. Yang, Y.Y. Chang, D.Y. Wang, D.Y. Lin, W.T. Wu, Mechanical properties of nano-structured Ti-Si-N film synthesized by cathodic arc evaporation, Journal of Alloys and Compounds 440 (2007) 375-379.
[8] S.C. Tjong, H. Chen, Nanocrystalline materials and coatings, Materials Science and Engineering R 45 (2004) 1-88.
[9] S. Zhang, N. Ali, Nanocomposite Thin Films and Coatings, Imperial College Press, London, 2007.
[10] S. Veprek, M.G.J. Veprek-Heijman, P. Karvankova, J. Prochazka, Different approaches to superhard coatings and nanocomposites, Thin Solid Films 476 (2005) 1-29.
[11] C. Donnet, A. Erdemir, Historical developments and new trends in tribological and solid lubricant coatings, Surface and Coatings Technology 180-181 (2004) 76-84.
[12] A.A. Voevodin, J.S. Zabinski, Nanocomposite and nanostructured tribological materials for space applications, Composites Science and Technology 65 (2005) 741-748.
[13] P. Holubar, M. Jilek, M. Sima, Present and possible future applications of superhard nanocomposite coatings, Surface and Coatings Technology 133-134 (2000) 145-151.
[14] D. Rafaja, A. Poklad, V. Klemm, G. Schreiber, D. Heger, M. Sima, Microstructure and hardness of nanocrystalline $Ti_{1-x-y}Al_xSi_yN$ thin films, Materials Science and Engineering A462 (2007) 279-282.
[15] S. Carvalho, E. Ribeiro, L. Rebouta, C. Tavares, J.P. Mendonca, A. Caetano Monteiro, N.J.M. Carvalho, J.Th. M. De Hosson, A. Cavaleiro, Microstructure, mechanical properties and cutting performance of superhard (Ti,SiAl)N nanocomposite films grown by d.c. reactive magnetron sputtering, Surface and Coatings Technology 177-178 (2004) 459-468.
[16] S. Veprek, Conventional and new approaches towards the design of novel superhard materials, Thin Solid Films 97 (1997) 15-22.
[17] S. Veprek, New development in superhard coatings: the superhard nanocrystalline-amorphous composites, Thin Solid Films 317 (1998) 449-454.
[18] D. Rafaja, A. Poklad, V. Klemm, G. Schreiber, D. Heger, M. Sima, M. Dopita, Some consequences of the partial crystallographic coherence between nanocrystalline domains in Ti-Al-N and Ti-Al-Si-N coatings, Thin Solid Films 514 (2006) 240-249.
[19] A.O. Sergici, N.X. Randall, Scratch testing of coatings, Advanced Materials and Processes 4 (2006) 1-3.
[20] Y. He, I. Apachitei, J. Zhou, T. Walstock, J. Duszczyk, Effect of prior plasma nitriding applied to a hot-work tool steel on the scratch-resistant properties of PACVD TiBN and TiCN coatings, Surface and Coatings Technology 201 (2006) 2534-2539.